Liquid Crystals

ISSN: 0267-8292 (Print) 1366-5855 (Online) Journal homepage: https://www.tandfonline.com/loi/tlct20

The influence of diluter system on polymer-stabilised blue-phase liquid crystals

Nejmettin Avci

To cite this article: Nejmettin Avci (2018) The influence of diluter system on polymer-stabilised blue-phase liquid crystals, Liquid Crystals, 45:3, 459-467, DOI: 10.1080/02678292.2017.1346825

To link to this article: https://doi.org/10.1080/02678292.2017.1346825

Published online: 03 Jul 2017.

LIQUID CRYSTALS, 2018
VOL. 45, NO. 3, 459–467
https://doi.org/10.1080/02678292.2017.1346825

Taylor & Francis
Taylor & Francis Group

The influence of diluter system on polymer-stabilised blue-phase liquid crystals

Nejmettin Avci[a,b]

[a]Faculty of Science, Department of Physics, Mugla Sitki Kocman University, Mugla, Turkey; [b]College of Optics and Photonics, University of Central Florida, Orlando, FL, USA

ABSTRACT

In the present work, diluter effects on the phase transition temperatures and electro-optical properties of the polymer-stabilised blue-phase liquid crystals with microsecond respond time have been carried out. The temperature range of polymer-stabilised blue-phase samples broadened over 50 K including room temperature. By increasing the concentration of diluter, the faster response time is obtained, but Kerr constant become smaller. These values are still two orders of magnitude larger than conventional Kerr materials such as nitrobenzene. The major bottleneck is the increased operating voltage. Hysteresis is sensitive to the diluter concentration and is slightly small for polymer network systems. For next-generation display technology, an optimal concentration of diluter plays a crucial role to a proper balance between response time and operation voltage.

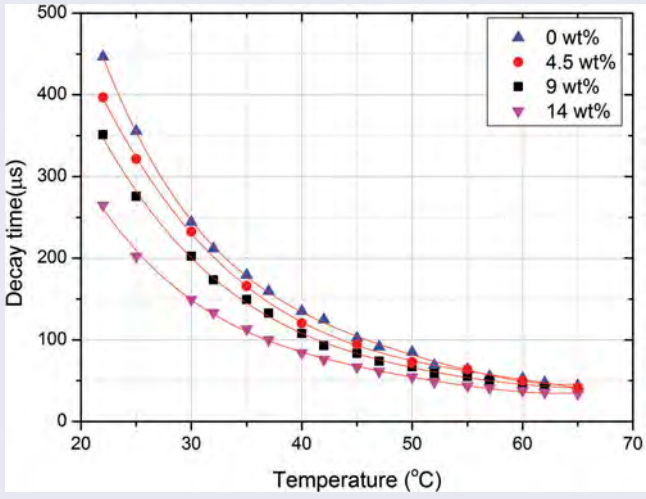

ARTICLE HISTORY
Received 29 March 2017
Accepted 21 June 2017

KEYWORDS
Polymer blue phase; liquid crystal; diluter; response time; Kerr constant

1. Introduction

Blue phases (BPs) are found in a fairly narrow temperature range between the high-temperature isotropic phase and the low-temperature chiral nematic phase of sufficiently short helical pitch [1,2]. BP is a coexistence of double-twist helical structure and defects (disclination lines) which tend to make the global structure less stable. Therefore, the thermal instability of BP is a major obstacle to their useful technological applications. There have been a variety of attempts to enlarge the temperature range of BPs. Among them, the first promising expansion of the BP temperature range was reported by Kikuchi et al. [3]. The photopolymerisation of a small amount of monomers in a BP state was selectively filled up the space in the disclination lattice, thereby reducing the free energy costs of the defects against temperature variation [3]. As a result, the temperature range of blue-phase liquid crystal (BPLC) was successfully extended to more than 100 K by means of a polymer network, including room temperature. It is referred to as polymer-stabilised blue phases (PSBPs). Besides polymer stabilisation, other methods for BP stabilisation involve the use of dimmer liquid crystal (LC) molecules with a large flexo-electric coefficient [4], nanoparticles with different diameters [5–9], hydrogen-bonded self-assembled LC complexes [10,11], T-shaped molecules [12], bent-shaped molecules [13–17] and binaphthyl derivatives [18].

CONTACT Nejmettin Avci navci@mu.edu.tr

Polymer-stabilised blue-phase liquid crystal (PSBPLC) has exhibited a number of intrinsic features in display applications, such as fast response time (in the sub-millisecond range) [19–22], optically isotropic at voltage-off state [23,24], alignment-free fabrication [24], wide viewing angle and cell gap insensitivity [23]. Nevertheless, their notable high driving voltage, electro-optical hysteresis and residual transmittance are the considerable bottleneck problems for display device applications [19–22,25]. Fast response time is probably the most attractive feature for BPLCs. Since it not only reduces motion blurs but also enables colour-sequential display using RGB LEDs, which eliminates the spatial colour filters [22]. By far, several methods have been implemented for reducing the response time. These methods include changing polymer ingredients [26,27], applying dual-frequency operation [28], employing longer exposure wavelength [29], applying electric field below the critical field [30] and increasing monomer concentration [29,31,32]. However, high monomer concentration results in the increased operation voltage. Xiang et al. [33] demonstrated a fast switching broad-temperature range electro-optical material by means of a BP-polymer-templated nematic. However, delicate fabrication processes of washing out unpolymerised components in the cell and refilling nematic LC must be performed in this method. Choi et al. demonstrated a method of enhancing response time by shortening the pitch of BPLC [34]. However, the solubility of chiral dopant in a nematic host is usually limited, and the decrease in pitch length affects the stability and formation of BP phase. The stated procedures have their own disadvantages. Some of them are expensive and time taking, while others are complicated.

To date, numerous proposed approaches have been demonstrated the electro-optical performance based on BPLC [3,4,7,13,14,16,18–39]. However, the diluter system which may have substantial effect on the properties of the PSBPLCs has rarely been investigated systematically [40–42]. Diluters have been employed for reducing the melting temperature and viscosity of a nematic material [43]. In the present paper, the effects of diluter systems on the thermal stability and the electro-optical properties of self-assembled nanostructured BPLC with polymer network were investigated. The electro-optical properties of the BPLCs compared with and without diluters. Higher diluter concentration improved the response time; however, its trade-offs were the decrease of Kerr constant and higher operating voltage. The Kerr constants of those were experimentally found up to two orders of magnitude larger than nitrobenzene. On the other hand, hysteresis was observed sensitive to the diluter concentration and was reduced by increasing temperature.

2. Experiment

To investigate the diluter effect on the PSBPLC, two kinds of the multicomponent mixtures comprising of rod-like nematic LCs were doped in the conventional BPLC system and were mixed systematically at different ratios. The stabilisation of the BPs was strongly dependent on the chemical structure of the monomer and fraction in the monomer mixture. For comparison, precursors were prepared in the same condition, as listed in Table 1.

The first nematic LC host was commercially known as E-7 (Merck). It is a multicomponent mixture comprising of 4-cyano-4′-pentylbiphenyl (51 wt%), 4-heptyl-4-cyanobi-phenyl (25 wt%), 4-octyloxy-4-cyanobiphenyl (16 wt%) and 4-pentyl-4-cyanoterphenyl (8 wt%). E-7 exhibits a nematic phase in the temperature interval from −10°C up to the transition to the isotropic phase at 59°C. E-7 has a birefringence $\Delta n = 0.2253$ at 20°C and $\lambda = 589.3$ nm, a positive dielectric anisotropy $\Delta\varepsilon = 13.89$ and a rotational viscosity $\gamma = 166$ m Pa.s at 20°C.

The second nematic LC host employed was HTG-135200 (HCCH, China). Its physical properties are $\Delta n = 0.205$ at $\lambda = 633$ nm, $\Delta\varepsilon = 100.3$ at 1kHz and 23°C and a rotational viscosity $\gamma = 1.2$ Pa.s (at 22°C); the clearing temperature is 96°C. The chemical structures are unavailable owing to commercial confidentiality. All chemical stuff was used without any further treatment.

A left-handed chiral dopant (S5011, HCCH) was added into each LC mixture to induce the BPs. Therefore, the BPLC sample transmitted the incident right-handed circular light in the voltage-off state. The helical twisting power of S5011 is dependent on the temperature and is approximately 120/μm. High concentration of chiral dopants results in the short pitch length. The chiral pitches were limited in a specific region by adjusting the chiral concentration. Since the electro-optical performance of PSBPLC is related to the

Table 1. The constituent fractions of the materials in order to prepare PSBPs.

Precursors	HTG-135200 + E-7 (wt %)	S5011 (wt%)	RM257 (wt%)	TMPTA (wt%)
0 wt%	85.50	4.50	5.00	5.00
4.5 wt%	85.50	4.50	5.02	4.98
9 wt%	85.44	4.56	5.00	5.00
14 wt%	84.40	5.60	5.01	4.99

pitch length. To broaden the temperature range of the BP, UV-curable monomers were used: 2-methyl-1,4-phenylene bis(4-(3-(acryloyloxy)propoxy) benzoate (RM257, Merck) and 1,1,1-trimethylolpropane triacrylate (TMPTA, Sigma Aldrich). The refractive indices for ordinary and extraordinary light of RM257 are $n_0 = 1.508$ and $n_e = 1.687$, respectively. The phase sequence of RM257 is the crystal–(70°C)–nematic–(120°C)–isotropic. RM257 is a di-acrylate monomer. TMPTA was added as a photocrosslinking agent to introduce rigidity to the cells. TMPTA is a tri-functional monomer. Any photoinitiator was not employed in this study. The total concentration of RM257 and TMPTA was fixed at 10% by weight. The BPLC/monomers mixtures were mechanically mixed at higher than the clearing point of the LC in order to form a homogeneous mixture for several times.

After homogeneous blending, each precursor was heated up to a temperature slightly higher than the isotropic phase to dissolve all components and then it was inserted into an empty in-plane-switching (IPS) cell without polyimide alignment layer at the isotropic state by means of capillary force. The BP does not require any surface treatment for alignment of LCs, since, it is optically isotropic. To measure the electro-optical properties of the materials, the top substrate of the IPS cells was a plain glass, but the bottom substrate was coated with comb-type interdigitated indium tin oxide (ITO) electrodes. The electrode distance was 12 μm. The ITO electrode was 8 μm wide. The cell thicknesses of IPS cells were controlled between 7.34 and 7.5 μm by glass spacer balls to separate substrates. The cell thickness was measured by the standard interferometric method. The temperature was carefully controlled by a Linkam hot stage LTS350 and a controller TMS94 with an accuracy of 0.1°C owing to the narrow temperature range of the BPs. The cells were stayed at thermal balance for 10 min, and then, they were cooled down from the isotropic phase to chiral nematic phase at a cooling rate of 0.5°C/min to observe the phase transition temperatures. After several thermal recycles, the cells were irradiated (from the plain glass substrate side at normal incidence) by UV light with a central wavelength of 365 nm (L2859–01, Hamamatsu Photonics LC6) at an intensity of ~8 mW/cm^2 for 30 min to stabilise the BPLC. This dosage is suitable to stabilise the BPLC composite system. After polymerisation, the samples were cooled to room temperature. The polymer chains were selectively concentrated in the disclination lines. As result, nanostructured PSBPLC composite was self-assembled. The phase transition temperatures and the optical texture of each sample were determined from a reflective polarising optical microscopy (POM) equipped with a commercial hotplate (Linkam TMS 94). The samples exhibited BPs during heating and cooling processes. Figure 1 shows the platelet textures of the samples observed under the POM in the reflective mode at room temperature, which exhibit that the samples were successfully polymer stabilised. Their phase transition temperatures were listed in Table 2.

As shown in Table 2, every mixture was found to exhibit PSBPLCs, even though the concentration range of chiral dopant and the temperature range were different. The clearing point of the precursors decreases with increasing the proportion of E-7 in the mixture, as a result of the low clearing point of E-7 mixture. The BPs existed over temperature range of $\sim 7 - 10^{\circ}$C without UV irradiation [7–18,44,45], which is wider than that over which typical BPs are normally found in a very narrow (~1°C) temperature range [1,2]. According to previous study, smaller dielectric anisotropy induced BPs in a wide temperature range [46]. The obtained results in this study are consistent with that. After formation of the polymer network, the clearing temperature is above 72°C, i.e. near to the clearing point of the respective mixture without any monomer, and the BP is now stable from below 22°C up to the clearing temperature. Therefore, the temperature range of PSBPLC samples reported in this study was extended to more than 50°C.

Figure 2 depicts the experimental setup. To characterise the electro-optical properties, a linearly polarised He–Ne laser (about 1mW at $\lambda = 633$ nm) was employed as a light source. The IPS cell was placed between a pair of crossed polarisers. To maximise the transmittance, azimuthal angle of the striped electrode was adjusted at an angle of 45° with respect to the plane of polarisation of the polariser. The transmitted light intensity was measured by a photodetector (New Focus Model 2031) connected to an oscilloscope (Tektronix TDS-2014). The samples were driven by a square-wave electric field with a frequency of 1 kHz put through an amplifier (FLC electronics, model F20) and was saved digitally by a LabView data acquisition system. The voltage ramping rate was 100ms. In the IPS cell, the electric field-induced birefringence was in the lateral direction to the plane of the substrate. The voltage-dependent transmitted light was focused by a lens to collect most of the diffraction orders into the photodetector.

3. Results and discussion

In the absence of an external electric field, PSBPLCs are optically isotropic owing to their cubic structure.

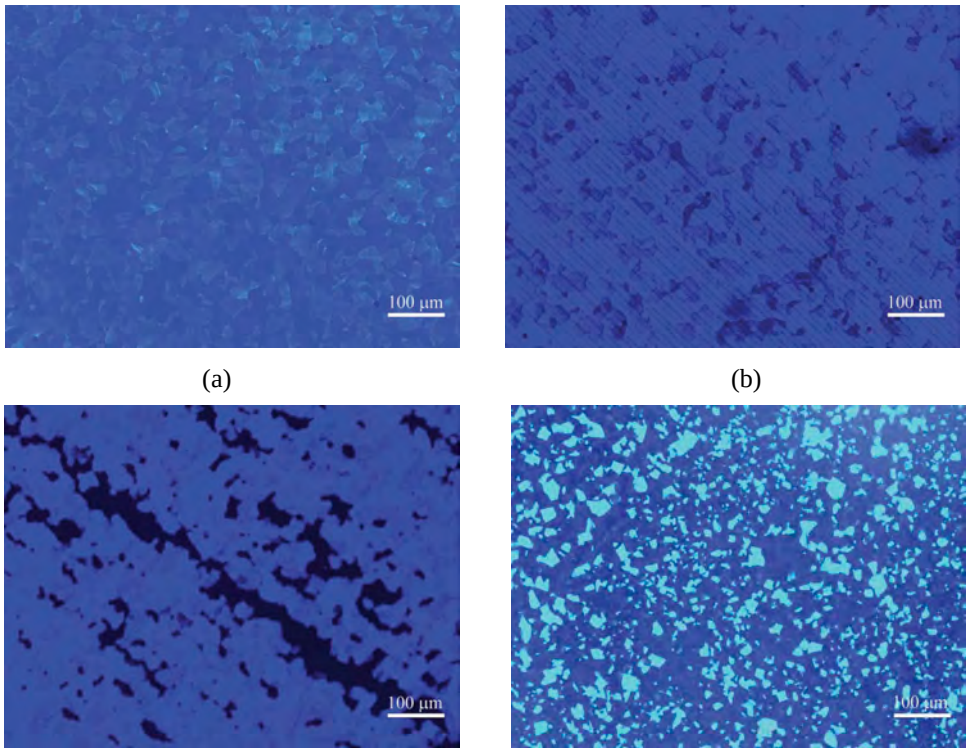

Figure 1. (Colour online) Micro-textures of samples observed under a polarising optical microscope with two crossed linear polarisers at room temperature (a) 0 wt% (the cell gap = 7.55 µm), (b) 4.5 wt% (the cell gap = 7.38 µm), (c) 9 wt% (the cell gap = 7.45 µm), (d) 14 wt% (the cell gap = 7.34 µm).

Table 2. Phase transition temperatures of BPLC mixtures (before and after photo-stabilisation) are determined by polarising optical microscope studies.

Before photo-stabilisation				
Samples	Cholesteric blue phase (°C)	Blue phase isotropic (°C)	Isotropic blue phase (°C)	Blue phase cholesteric phase (°C)
0 wt%	70.6	72.6	72	67.8
4.5 wt%	57.4	67.9	67.0	59.9
9 wt%	52.5	56.9	55.8	50.6
14 wt%	46.9	53.4	52.6	43.7
After photo-stabilisation				
Samples	Cholesteric blue phase (°C)	Blue phase isotropic (°C)	Isotropic blue phase (°C)	Blue phase cholesteric phase (°C)
0 wt%	Lower than 22	82.1	81.3	Lower than 22
4.5 wt%	Lower than 22	81.2	80.3	Lower than 22
9 wt%	Lower than 22	77.8	76.5	Lower than 22
14 wt%	Lower than 22	73.5	72.8	Lower than 22

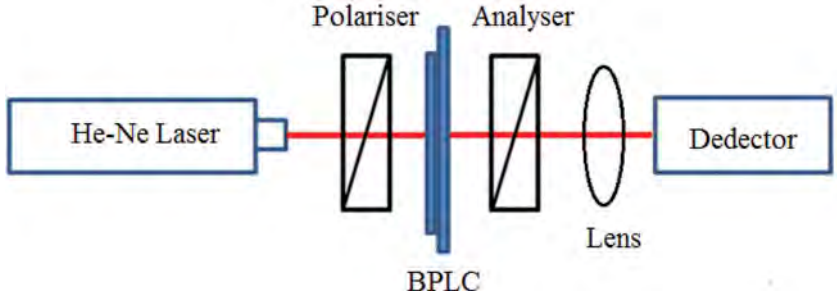

Figure 2. (Colour online) Experimental setup for electro-optic measurement of the IPS cell.

However, a birefringence can be induced by the application of the electric field due to a distortion of the cubic lattice of PSBPLCs. Therefore, the electro-optical properties of the PSBPLC were measured at different temperatures. Figure 3 demonstrates the normalised voltage-dependent transmittance curves (VT) by ascending and descending voltage operation cycles from 22°C to 62°C for 4.5 wt% of E-7 host in the precursors. These data may be approximately described by the relative transmitted intensity through a uniaxially birefringent slab:

$$T_{\mathrm{nor}} = \sin^2(2\Psi)\sin^2\left(\frac{\pi\Delta n_{\mathrm{induced}}(V)d}{\lambda}\right). \qquad (1)$$

Here, $\Delta n_{\mathrm{induced}}$ is the induced birefringence at a particular applied electric field strength and Ψ is the angle of the induced, in-plane, optic axis with respect to the polariser or analyser crossed axis ($\Psi = 45^\circ$ in this experiment). Here, the transmission was normalised to that of two parallel polarisers. The transmission gradually increased with increasing voltage, reaching a maximum value. Operating voltage (V_{on}) is defined as a voltage at the maximum transmittance of the VT curve. During backward sweep of voltage, the transmission became smaller but along a different way. As the temperature increases, V_{on} increases, as can be seen in Figure 4. This process was repeated for other samples.

As shown in Figure 4, one may see that the operating voltage increases with increasing temperature. Additionally, the required operating voltage increases as the concentration of E-7 host in the precursors increases. In the precursors without E-7 host, operating voltage was found to be 77 V at room temperature. On the other hand, the presence of 14 wt% E-7 in the precursors operating voltage was determined to be 95 V. In consequence, the peak driving voltage increases with increasing concentration of E-7 host in the compound. This phenomenon may result from the fact that the dielectric anisotropy of PSBPLC decreases with the presence of E-7.

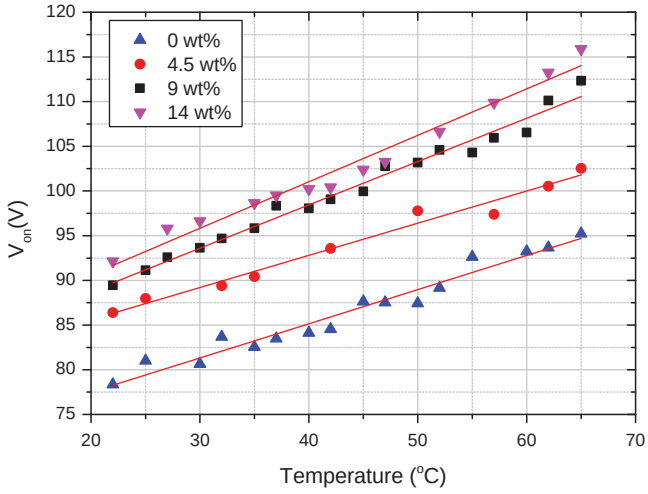

Figure 4. (Colour online) The operating voltage as a function of temperature for different concentrations of E-7 compound. Continuous lines are drawn as a guide to the eye.

According to Lichtenecker mixing rule, dielectric anisotropy ($\Delta\varepsilon_m$) of a binary mixture of LC can be written as follows [47]:

$$\log(\Delta\varepsilon_m) = \phi_1\log(\Delta\varepsilon_1) + (1-\phi_1)\log(\Delta\varepsilon_2), \qquad (2)$$

where $\Delta\varepsilon_1$ and $\Delta\varepsilon_2$ are dielectric anisotropy of the two components and ϕ_1 is the volume fraction of component. Substituting $\Delta\varepsilon_1 = 14$, $\Delta\varepsilon_2 = 100.3$ and $\phi_1 = 0.045$ into Equation (2), we can find $\Delta\varepsilon_m = 90.6$.

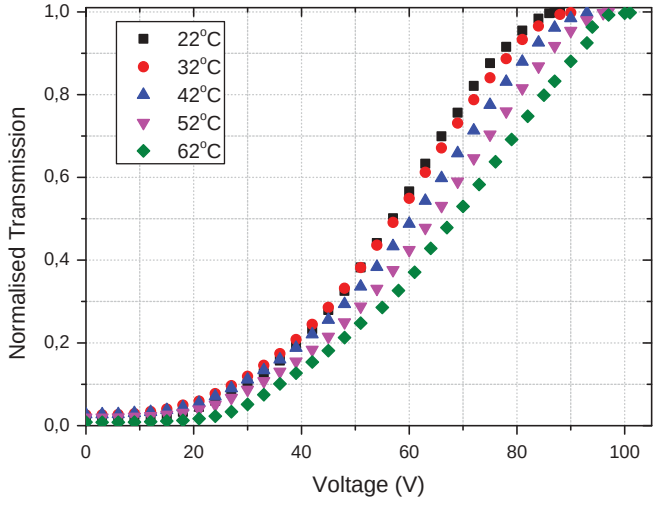

Figure 3. (Colour online) Measured V–T curves in an IPS cell at different temperatures using the experimental setup for 4.5 wt% of E-7 compound, IPS cell:cell gap = 7.38 µm, electrode gap = 12 µm and electrode width = 8 µm.

Adding in place of $\Delta\varepsilon_1 = 14$, $\Delta\varepsilon_2 = 100.3$ and $\phi_1 = 0.09$ into Equation (2), we can obtain $\Delta\varepsilon_m = 83.3$. And using in turn $\Delta\varepsilon_1 = 14$, $\Delta\varepsilon_2 = 100.3$ and $\phi_1 = 0.145$ into Equation (2), then we can find $\Delta\varepsilon_m = 75.2$.

It is believed that a large Kerr constant is observed for nematic LCs just above the nematic–isotropic phase transition temperature [48]. This is owing to short-range nematic-like order originated from orientational fluctuation in the isotropic liquid. Macroscopically, BPLC is an isotropic Kerr medium when there is no external electric field present. When electric field increases, the BPLC becomes anisotropic along the electric field direction. The refractive index change follows the Kerr effect in the low field region but gradually saturates as the electric field keeps increasing, which can be well explained by an extended Kerr effect [49]. The $\Delta n_{\text{induced}}$ in the weak field region is related to E, wavelength λ and Kerr constant K as shown below:

$$\Delta n_{\text{induced}} = \lambda K E^2. \tag{3}$$

According to the extended Kerr effect, the $\Delta n_{\text{induced}}$ of PSBPLCs is related to the electric field [49].

$$\Delta n_{\text{induced}}(E) = \Delta n_s \left(1 - \exp\left[-\left(\frac{E}{E_s}\right)^2\right]\right), \tag{4}$$

where Δn_s is the saturated induced birefringence and E_s is the saturation electric field. In the weak field region ($E \ll E_s$), the Kerr constant is derived as follows:

$$K \approx \frac{\Delta n_s}{\lambda {E_s}^2}. \tag{5}$$

Based on Equation (4), the Kerr constant is obtained by fitting the VT curves with the extended Kerr effect model, since the $\Delta n_{\text{induced}}$ should be saturated in the strong electric field. Figure 5 shows the Kerr constant consisting of different E-7 concentrations in the systems. In the precursors without E-7 host, the Kerr constant was found to be $8.5 \times 10^{-9}\text{V}^{-2}\text{m}$ at room temperature. By contrast, in the case of the precursors containing 14 wt% of E-7 host, the Kerr constant was found to be $5 \times 10^{-9}\text{V}^{-2}\text{m}$. As the concentration of E-7 in the precursors increases, the Kerr constant of PSBPLC decreases. The Kerr constant is proportional to $\Delta\varepsilon$ [50].

It indicates that $\Delta\varepsilon$ of the precursors decreases with increasing wt% of E-7 compound. Furthermore, an increase in required applied voltage corresponds to a decrease in Kerr constant. Nitrobenzene in a liquid state is known to show large Kerr constants, $K = 2\sim4 \times 10^{-12}\text{V}^{-2}\text{m}$. However, the values of the Kerr constant in the precursors are the order of

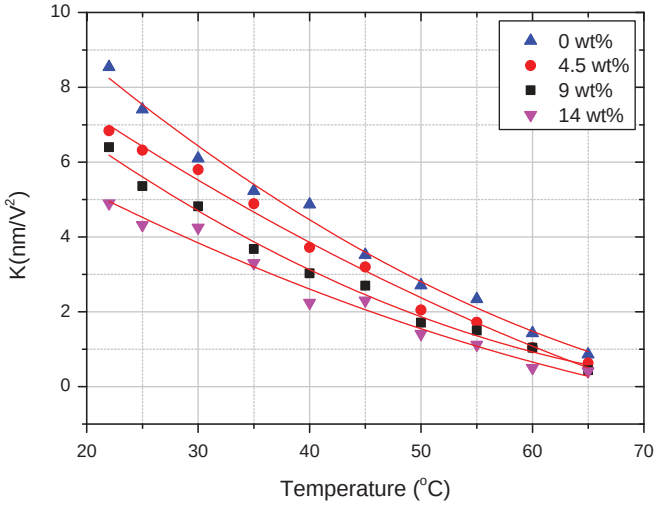

Figure 5. (Colour online) Temperature dependence of Kerr coefficient of PSBPs for different concentrations of E-7 compound. The lines are guides to the eyes.

$10^{-10} - 10^{-9}\text{V}^{-2}\text{m}$, which is about 100∼1000 times as large as the Kerr constant of polar liquid like nitrobenzene [51]. This value is comparable with that in a PSBPLC [26–28,31–34,36,37,40–42]. We can infer that the dielectric anisotropy of the system may be one of the reasons for decreasing the Kerr constant.

Microsecond grey-to-grey response time is one of the major properties of BPLC in comparison with conventional nematic LCs. Decay and rise times can be expressed, respectively, as follows:

$$T_{\text{decay}} = \frac{\gamma_1}{{E_c}^2 \varepsilon_o \Delta\varepsilon}. \tag{6}$$

$$T_{\text{rise}} = \frac{T_{\text{decay}}}{(V/V_c)^2 - 1}. \tag{7}$$

Here, V_c is the critical voltage in order to unwind the BPLC pitches, γ_1 stands for the rotational viscosity and E_c is the critical electric field.

Figure 6 displays the temperature dependence of the decay and rise processes for the PSBPs consisting of various ratios of LC hosts, respectively. The decay and rise times were determined from 90% to 10% transmittance change. All the measurements were conducted at different temperatures. As seen in Figure 6, the decay time is slower than the rise process. In addition, the rise and decay processes decrease with increasing temperature, since the rise time is affected by the dielectric anisotropy of the LC host. In the absence of E-7 host in the PSBP, the response time was found to be 447 μs in the decay process and 250 μs in the rise process at room temperature. In the case of the PSBP comprising of 14 wt% of E-7 host, the response time was found to

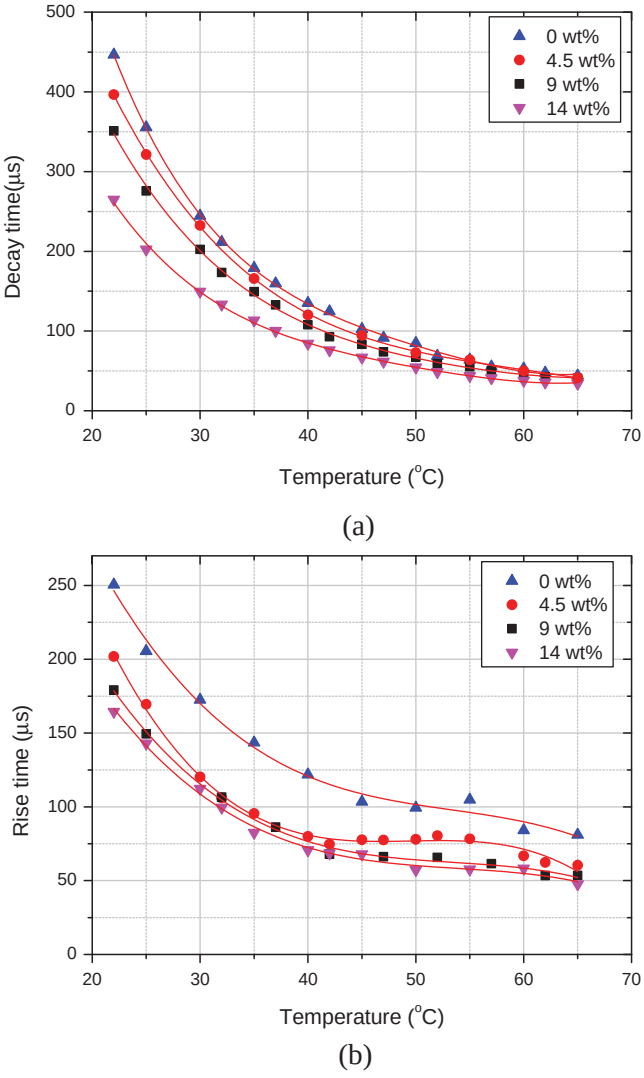

Figure 6. (Colour online) Temperature dependence of electro-optical response time for different concentrations of E-7 compound (a) decay time and (b) rise time. Continuous lines are drawn as a guide to the eye.

be 265 μs in the decay process and 163 μs in the rise process at room temperature (in the region of local director reorientation).

On the other hand, the response time of the PSBP containing 14 wt% of E-7 showed 63 μs in the decay process and 40 μs in the rise process at 65°C. Over a wide temperature, the response times were of the order of microseconds. This is much faster than those of nematic LCs, which are typically about 10–100 ms. Namely, doping 14 wt% of E-7 in the precursor, the decay time is improved by ~2× with respect to 0 wt% of E-7 in the precursor at room temperature and resulted in diminishing the effective rotational viscosity of the material system. These times are comparable with those published in the literature [3,7,16,25–42]. Therefore, the performance of the PSBPLC was enhanced. It is believed that the fast response time originates from the short pitch length, LC host and strong cross-linking polymer network [19–22]. This indicates that our precursors form strong polymer network. As a result, it is found that the response time makes shorter with increasing ratios of E-7 host in the precursors. Higher operating voltage is a trade-off effect for display application.

Hysteresis is a key issue that affects the grey scale in LC displays, and it should be minimised prior to the wide application of PSBPLCs [21,25]. To measure the hysteresis of our IPS devices, the IPS devices were driven by increasing the applied voltage upwards to V_{on} and then gradually decreasing downwards to zero. The hysteresis is defined by the voltage difference

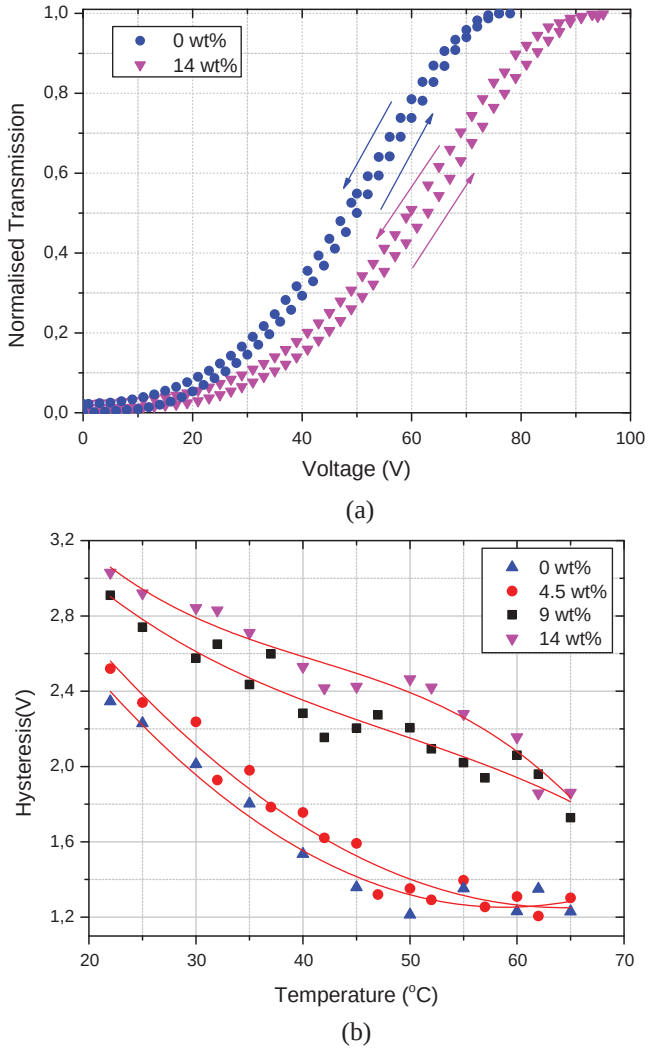

Figure 7. (Colour online) (a) Measured hysteresis loops for different concentrations of E-7 compound at room temperature and (b) temperature dependence of voltage hysteresis for different concentrations of E-7 compound. The lines are guides to the eyes.

between the upward and downward scans at half of the peak transmittance. Higher operating voltage gives rise to a more discernible hysteresis, which is ascribed to the lattice distortions of the PSBPLC.

Figure 7 demonstrates the hysteresis of PSBPLCs obtained under different LC host compounds. When the concentration of E-7 host in the precursors changes from 0% to 14%, the hysteresis increases from 2.35 to 3.07 V at room temperature. Additionally, the hysteresis makes smaller with increasing temperature. In other words, hysteresis is relatively sensitive to temperature and the diluter concentration. The reduction in hysteresis may cause the reduction in rotational viscosity with an increase in temperature [25]. Low rotational viscosity gives rise to rapid relaxation which decreases hysteresis and Kerr constant. This decrease in hysteresis can make PSBPLCs beneficial in display devices. The composition of the PSBPLC samples requires finding a reasonable compromise to attain faster electro-optical response time at low hysteresis.

4. Conclusion

In summary, the effects of the diluters and composition on the electro-optic performance of PSBPLC with a wide temperature range including room temperature have been investigated. It was found that increasing the diluter concentration (E-7) leads to faster response time, smaller hysteresis, higher driving voltage and lower Kerr constant. In addition, the experimental results indicate that a small amount of diluter slightly decreases the dielectric anisotropy but dramatically reduces the viscosity of the employed material system. Therefore, an optimal concentration of diluter should be taken into account for optimising the total performance of the BPLC systems.

Acknowledgements

This research was supported by grants from the Scientific and Technological Research Council of Turkey (TUBITAK) to N. Avci. The author also gratefully acknowledges Prof. Shin-Tson Wu of the University of Central Florida for technical assistance and providing the liquid crystal material and instruments.

Disclosure statement

No potential conflict of interest was reported by the author.

Funding

This research was supported by grants from the Scientific and Technological Research Council of Turkey (TUBITAK) to N. Avci

References

[1] Reinitzer F. Beiträge zur Kenntniss des Cholesterins. Monatshefte Für Chemie (Wein). 1888;9:421–441. Translation: Contributions to the understanding of cholesterol. Liq Cryst. 1989;5:7–18. DOI:10.1080/02678298908026349
[2] Crooker PP. Blue phases. In: Kitzerow H-S, Bahr C, editors. Chirality of liquid crystals. New York: Springer-Verlag; 2011. p. 186–222.
[3] Kikuchi H, Yokota M, Hisakado Y, et al. Polymer stabilized liquid crystal blue phases. Nat Mater. 2002;1:64–68. DOI:10.1038/nmat712
[4] Coles HJ, Pivnenko MN. Liquid crystal blue phases with a wide temperature range. Nat Mater. 2005;436:997–1000. DOI:10.1038/nature03932
[5] Dierking I, Blenkhorn W, Credland E, et al. Stabilising liquid crystalline blue phases. Soft Matter. 2012;8:4355–4362. DOI:10.1039/c2sm07155j
[6] Yoshida H, Tanaka Y, Kawamoto K, et al. Nanoparticle-stabilized cholesteric blue phases. Appl Phys Express. 2009;2:121501. DOI:10.1143/APEX.2.121501
[7] Wang L, He W, Xiao X, et al. Hysteresis free blue phase liquid crystal stabilized by ZnS nanoparticles. Small. 2012;8:2189–2193. DOI:10.1002/smll.201200052
[8] Lavrič M, Cordoyiannis G, Kralj S, et al. Effect of anisotropic MoS_2 nanoparticles on the blue phase range of a chiral liquid crystal. Appl Opt. 2013;52:47–52. DOI:10.1364/AO.52.000E47
[9] Karatairi E, Rožič B, Kutnjak Z, et al. Nanoparticle-induced widening of the temperature range of liquid-crystalline blue phases. Phys Rev E. 2010;81:041703-1-5. DOI:10.1103/PhysRevE.81.041703
[10] He W, Pan G, Yang Z, et al. Wide blue phase range in a hydrogen-bonded self-assembled complex of chiral fluoro-substituted benzoic acid and pyridine derivative. Adv Mater. 2009;21:2050–2053. DOI:10.1002/adma.200802927
[11] Gvozdovskyy I. 'Blue phases' of highly chiral thermotropic liquid crystals with a wide range of near-room temperature. Liq Cryst. 2015;42:1391–1404. DOI:10.1080/02678292.2015.1053001
[12] Yoshizawa A, Sato M, Rokunohe J. A blue phase observed for a novel chiral compound possessing molecular biaxiality. J Mater Chem. 2005;15:3285–3290. DOI:10.1039/B506167A
[13] Taushanoff S, Le KV, Williams J, et al. Stable amorphous blue phase of bent-core nematic liquid crystals doped with a chiral material. J Mater Chem. 2010;20:5893–5898. DOI:10.1039/c0jm00690d
[14] Lee M, Hur S-T, Higuchi H, et al. Liquid crystalline blue phase I observed for a bent-core molecule and its electro-optical performance. J Mater Chem. 2010;20:5813–5816. DOI:10.1039/C0JM01087A
[15] Wang H, Zheng Z, Shen D. Blue phase liquid crystals induced by bent-shaped molecules based on 1,3,4-oxadiazole derivatives. Liq Cryst. 2012;39:99–103. DOI:10.1080/02678292.2011.628704
[16] Park K-W, Gim M-J, Kim S, et al. Liquid-crystalline blue phase II system comprising a bent-core molecule with a wide stable temperature range. Appl Mater Interfaces. 2013;5:8025–8029. DOI:10.1021/am403109q

[17] Zheng Z, Shen D, Huang P. Wide blue phase range of chiral nematic liquid crystal doped with bent-shaped molecules. New J Phys. 2010;10:113018-1-10. DOI:10.1088/1367-2630/12/11/113018
[18] Yoshizawa A, Kogawa Y, Kobayashi K, et al. A binaphthyl derivative with a wide temperature range of a blue phase. J Mater Chem. 2009;19:5759–5764. DOI:10.1039/b902898f
[19] Yan J, Wu S-T. Polymer-stabilized blue phase liquid crystals: a tutorial [invited]. Opt Mater Express. 2011;1:1527–1535. DOI:10.1364/OME.1.001527
[20] Chen Y, Wu S-T. Recent advances on polymer-stabilized blue phase liquid crystal materials and devices. J Appl Polym Sci. 2014;131:40556. DOI:10.1002/app.40780
[21] Rao L, Ge Z, Wu S-T, et al. Low voltage blue-phase liquid crystal displays. Appl Phys Lett. 2009;95:231101. DOI:10.1063/1.3271771
[22] Yan J, Rao L, Jiao M, et al. Polymer-stabilized optically isotropic liquid crystals for next generation display and photonics applications. J Mater Chem. 2011;21:7870–7877. DOI:10.1039/c1jm10711a
[23] Ge Z, Rao L, Gauza S, et al. Modeling of blue phase liquid crystal displays. J Disp Technol. 2009;5:250–256. DOI:10.1109/JDT.2009.2022849
[24] Rao L, Ge Z, Gauza S, et al. Emerging liquid crystal displays based on the Kerr effect. Mol Cryst Liq Cryst. 2010;527:30–42. DOI:10.1080/15421406.2010.486600
[25] Chen K-M, Gauza S, Xianyu H, et al. Hysteresis effects in blue phase liquid crystals. J Disp Technol. 2010;6:318–322. DOI:10.1109/JDT.2010.2055039
[26] Zhu JL, Ni SB, Su Y, et al. The influence of polymer system on polymer-stabilised blue phase liquid crystals. Liq Cryst. 2014;41:891–896. DOI:10.1080/02678292.2014.882023
[27] Zhu JL, Ni SB, Song Y, et al. Improved Kerr constant and response time of polymer-stabilized blue phase liquid crystal with a reactive diluent. Appl Phys Lett. 2013;102:071104. DOI:10.1063/1.4793416
[28] Yabu S, Yoshida H, Lim G, et al. Dual frequency operation of a blue phase liquid crystal. Opt Mat Express. 2011;1(8):1577–1584. DOI:10.1364/OME.1.001577
[29] Oo T-N, Mizunuma T, Nagano Y, et al. Effects of monomer/liquid crystal compositions on electro-optical properties of polymer-stabilized blue phase liquid crystal. Opt Mat Express. 2011;1:1502–1510. DOI:10.1364/OME.1.001502
[30] Yan J, Chen Y, Wu S-T, et al. Dynamic response of a polymer-stabilized blue-phase liquid crystal. J Appl Phys. 2012;111:063103. DOI:10.1063/1.3694733
[31] Kikuchi H, Hisakado Y, Uchida K, et al. Fast electro-optical effect in polymer-stabilized blue phases. Proc SPIE. 2004;5518:182–189. DOI:10.1117/12.555975
[32] Yoshida H, Kikuchi H, Nagamura T, et al. Large electro-optic Kerr effect in polymer-stabilized liquid-crystalline blue phases. Adv Mater. 2005;17:96–98. DOI:10.1002/adma.200400639
[33] Xiang J, Lavrentovich OD. Blue-phase-polymer-templated nematic with sub-millisecond broad-temperature range electro-optic switching. Appl Phys Lett. 2013;103:051112-1-4. DOI:10.1063/1.4817724
[34] Choi H, Higuchi H, Kikuchi H. Electro-optic response of liquid crystalline blue phases with different chiral pitches. Soft Matter. 2011;7:4252–4256. DOI:10.1039/c1sm05098b
[35] Chen KM, Gauza S, Wu S-T, et al. Submillisecond gray-level response time of a polymer-stabilized blue-phase liquid crystal. J Disp Technol. 2010;6:49–51. DOI:10.1109/JDT.2009.2037981
[36] Rao L, Yan J, Wu S-T, et al. A large Kerr constant polymer-stabilized blue phase liquid crystal. Appl Phys Lett. 2011;98:081109. DOI:10.1063/1.3559614
[37] Chen Y, Xu D, Wu S-T, et al. A low voltage and sub-millisecond-response polymer-stabilized blue phase liquid crystal. Appl Phys Lett. 2013;102:141116. DOI:10.1063/1.4802090
[38] Xu D, Yan J, Yuan J, et al. Electro-optic response of polymer-stabilized blue phase liquid crystals. Appl Phys Lett. 2014;105:011119. DOI:10.1063/1.4890031
[39] Yan J, Wu S-T. Effect of polymer concentration and composition on blue phase liquid crystals. J Display Tech. 2011;7:490–493. DOI:10.1109/JDT.2011.2159091
[40] Chen Y, Yan J, Schadt M, et al. Diluter effects on polymer-stabilized blue phase liquid crystals. J Display Technol. 2013;9(7):592–597. DOI:10.1109/JDT.2013.2254109
[41] Peng F, Chen Y, Yuan J, et al. Low temperature and high frequency effects on blue phase liquid crystals. J Display Technol. 2014;45:164–167. DOI:10.1002/j.2168-0159.2014.tb00045.x
[42] Peng F, Chen Y, Yuan J, et al. Low temperature and high frequency effects on polymer-stabilized blue phase liquid crystals with large dielectric anisotropy. J Mater Chem C. 2014;2:3597–3601. DOI:10.1039/c4tc00115j
[43] Song Q, Gauza S, Sun J, et al. Diluters' effects on high Δn and low-viscosity negative Δε terphenyl liquid crystals. Liq Cryst. 2009;36:865–872. DOI:10.1080/02678290903100521
[44] Kishikawa K, Watanabe T, Kohri M, et al. Effect of the number of chiral mesogenic units and their spatial arrangement in dopant molecules on the stabilisation of blue phases. Liq Cryst. 2014;41(6):839–849. DOI:10.1080/02678292.2014.885599
[45] Pawsey AC, Clegg PS. Colloidal particles in blue phase liquid crystals. Soft Mater. 2015;11:3304–3312. DOI:10.1039/C4SM02131B
[46] Chen HY, Liu HH, Lai JL, et al. Relation between physical parameters and thermal stability of liquid-crystal blue phase. Appl Phys Lett. 2010;97:181919. DOI:10.1063/1.3509413
[47] Lichtenecker K, Rother K. Die Herleitung des logarithmischenMis-chungsgesetzes aus allgemeinen Prinzipien der stationären Strömung. Phys Z. 1931;32:255–260.
[48] Li BX, Borshch V, Shiyanovskii SV, et al. Kerr effect at high electric field in the isotropic phase of mesogenic materials. Phys Rev E. 2015;92(5):050501. DOI:10.1103/PhysRevE.92.050501
[49] Yan J, Cheng HC, Gauza S, et al. Extended Kerr effect of polymer-stabilized blue-phase liquid crystals. Appl Phys Lett. 2010;96:071105. DOI:10.1063/1.3318288
[50] Gerber PR. Electro-optical effects of a small-pitch blue-phase system. Mol Cryst Liq Cryst. 1985;116:197–206. DOI:10.1080/00268948508074573
[51] Hecht E. Optics. Reading. MA: Addison Wesley; 2002. p. 318–320.